Structure of binary polymer blends: Multiple time step hybrid Monte Carlo simulations and self-consistent integral-equation theory

Dmitry G. Gromov and Juan J. de Pablo
Department of Chemical Engineering, University of Wisconsin-Madison, Madison, Wisconsin 53706

(Received 31 May 1995; accepted 31 July 1995)

A newly developed self-consistent formulation of the polymer reference interaction site model (PRISM) theory is used to predict the structure of binary polymer blends. Theoretical radial distribution functions are compared to those obtained from hybrid Monte Carlo simulations of mixtures of Lennard-Jones chains. A multiple time step method is implemented to increase the efficiency of the simulations. We examine both the cases of atomic and molecular closures and consider both conventional and self-consistent PRISM. We find that, overall, theoretical distribution functions are in good agreement with simulation. © *1995 American Institute of Physics.*

I. INTRODUCTION

It is generally accepted that local molecular structure plays a crucial role in determining the thermodynamic properties of pure simple liquids and their mixtures. Accordingly, the theory of simple liquids has received a great deal of attention over the last three decades.[1,2] More recently, some of the methods originally developed for such liquids have been applied to polymers, which had traditionally been studied by invoking lattice representations of the system. Computer simulations of polymeric fluids have also received increasing amounts of attention in recent years, and the focus of such calculations has gradually shifted from studies on a lattice to a continuum.

The integral-equation formulation of Schweizer and Curro (PRISM) has permitted calculation of the structure of pure homopolymers[3–5] and blends.[6–8] Unfortunately, the predictions of such a theory have only been compared to simulations of pure polymers. We note, however, that Stevenson *et al.*[9] and de Pablo[10] have very recently conducted limited simulations of polymer blends in attempts to examine PRISM's accuracy for mixtures. The PRISM theory of Schweizer and Curro requires information about the intramolecular structure of the molecules. Originally, such information was obtained either by resorting to other theories of polymers or directly from molecular simulations. A new self-consistent formulation, however, has allowed complete first-principles predictions of the structure of pure homopolymers.[11] Part of the purpose of this work is to examine the accuracy of self-consistent PRISM for blends by comparing theoretical distribution functions to those obtained from molecular simulations.

In this paper we apply a new multiple time step hybrid Monte Carlo method to determine the exact structure of freely jointed Lennard-Jones chains over a wide range of LJ parameters, compositions, and chain lengths. We present data on the efficiency of the proposed simulation method. We apply the original PRISM theory as well as its fully self-consistent formulation to calculate the intra- and intermolecular structure of pure polymers and binary polymer blends. Our work is different and complements that of Stevenson *et al.*[9] in several respects. First, these authors employ a somewhat different molecular model. Second, these authors address the validity of PRISM when a simulated intramolecular structure is employed. Third, they limit their calculations to purely repulsive blends. In contrast, we examine the accuracy of a self-consistent theory and address the effects of attractive forces on the structure of binary polymer blends using both atomic and molecular closures.

II. MOLECULAR MODEL

The polymers studied in this work consist of fully flexible chains of Lennard-Jones sites. Adjacent sites on the chains are connected by finitely extensible nonlinear elastic (FENE) (Ref. 12) connectors. The FENE potential-energy function describing the interactions between ''covalently'' bonded beads is given by

$$U^{\mathrm{cov}}(r) = -\frac{1}{2} H Q_0^2 \ln\left(1 - \frac{r^2}{Q_0^2}\right) + U^{\mathrm{LJ}}(r), \tag{1}$$

where H is a force constant, Q_0 is the maximum extensibility of the springs, and $U^{\mathrm{LJ}}(r)$ is the Lennard-Jones potential given by

$$U^{\mathrm{LJ}}(r) = 4\epsilon\left[\left(\frac{\sigma}{r}\right)^{12} - \left(\frac{\sigma}{r}\right)^{6}\right]. \tag{2}$$

Each interaction site is characterized by three sets of Lennard-Jones parameters: one for covalently bonded interaction sites, one for interactions between beads that are not chemically bonded, and one for cross-interactions between different species. For this study we used $H=100$ and $Q_0=1.5$. These values lead to an average bond length of approximately 0.9σ (where σ is the Lennard-Jones size parameter). In other words, the chains can be viewed as a collection of slightly overlapping soft spheres of diameter σ. All beads on a chain interact with each other and with those on other chains through a Lennard-Jones potential energy function [Eq. (2)]. The total potential energy of a polymer melt having a total number of beads equal to N is given by

$$U(r^{3N}) = \sum_{i,j\{\text{nonbonded}\}} U_{ij}^{\mathrm{LJ}}(r_{ij}) + \sum_{k,l\{\text{bonded}\}} [U_{kl}^{\mathrm{LJ}}(r_{kl}) + U_{kl}^{\mathrm{FENE}}(r_{kl})]. \tag{3}$$

This model is simple and yet flexible enough to allow us to study blends having different degrees of dissimilarity. We analyze primarily two different types of dissimilarity; an ''energy'' dissimilarity, using the relations

$$\epsilon_{11} \neq \epsilon_{22} \neq \epsilon_{12} = \sqrt{\epsilon_{11}\epsilon_{22}}\,, \tag{4}$$

$$\sigma_{11} = \sigma_{22} = \sigma_{12}\,, \tag{5}$$

and a ''size'' dissimilarity, described by

$$\epsilon_{11} = \epsilon_{22} = \epsilon_{12}\,, \tag{6}$$

$$\sigma_{11} \neq \sigma_{22} \neq \sigma_{12} = \frac{\sigma_{11}+\sigma_{22}}{2}. \tag{7}$$

III. SIMULATION METHOD

Both molecular dynamics (MD) and Monte Carlo (MC) methods are commonly used for simulation of polymeric materials. However, computer simulations of dense polymer systems are notoriously difficult due to the lack of free volume at high densities and due to the limitations imposed by the chain connectivity. Much of the recent progress in the area of computer simulation of polymers can be attributed to the development of novel, polymer-specific simulation MC techniques.[13–17] These specific methods take into account the chain connectivity when new, trial configurations are proposed. For example, in a *continuum configurational bias* (CCB) method[13] a chain is cut at a random point and is then regrown, site by site, into its original length. This method has been shown to be superior to more conventional Monte Carlo techniques.[13,14] We believe that, for the case of intermediate chain lengths and low density, the CCB method is highly effective. Unfortunately, the efficiency of CCB method decreases drastically with chain length. For an exhaustive review of modern polymer simulation techniques, the reader is referred to Ref. 18. In this work we have therefore chosen to simulate dense polymer melts using a hybrid Monte Carlo method described below. For single chains in a mean field, however, we use CCB methods.

A. Multiple time step molecular dynamics method

Multiple time step variants of the molecular dynamics method are typically considerably faster than conventional MD. They are particularly efficient for systems that exhibit two or more very different time scales. The physical idea behind them is that the force acting on an interaction site i, $\mathbf{F}_i$, can be divided into a ''fast'' part (e.g., due to vibrational degrees of freedom) and a ''slow'' part (e.g., due to Lennard-Jones interactions between unbonded interaction sites). The use of different time steps for integration of slow and fast degrees of freedom has been suggested by various authors; speedup factors as high as 20–30 have been reported in the literature.[19,20] Recently, a new *reversible reference system propagator* algorithm (RESPA) has been proposed.[21] The main feature of RESPA that makes it attractive for our own work resides in its time reversibility. This property is crucial for using the algorithm in conjunction with hybrid Monte Carlo methods. The details of the proposed multiple time step molecular dynamics method as applied to polymers are given in Appendix A.

Some important concerns when doing MD simulations are the accuracy and stability of the algorithm. For many-body nonlinear systems, any two classical trajectories which are initially very close to each other will eventually diverge exponentially with time from one another according to their Lyapunov exponents.[22] Any small error associated with the finite-difference method will therefore cause a calculated trajectory to diverge from the true classical trajectory with which it is initially coincident.[23] In other words, due to the discretization in time, MD is subject to errors and instabilities set by the time step size and by the length of the simulation. Hybrid methods avoid these shortcomings of MD simulations.

B. Hybrid Monte Carlo method

Conventional Monte Carlo calculations are generally carried out by means of single-particle updates only. Updating more than one particle at a time typically results in a prohibitively low average acceptance probability. This implies large relaxation times and high autocorrelations. On the other hand, MD simulations require global moves. As mentioned above, however, the MD scheme is prone to errors and instabilities due to finite time step sizes.

The hybrid Monte Carlo (HMC) algorithm proposed by Duane *et al.*[24] combines the ease of calculation of trajectories (for all particles) of molecular dynamics methods but, as any Monte Carlo scheme, it is exact. The algorithm is unlike conventional MC methods because it involves global updates of positions for all interaction sites followed by an accept/reject decision for the whole configuration. It is also unlike any normal MD scheme because there are no discretization errors; in principle, the time step size δt in HMC can be large while keeping the method exact. The properties of HMC in the context of condensed-matter systems have been studied by Mehlig *et al.*[25] One global move in configurational space consists of integrating the system through phase space for a fixed time t using some arbitrary time discretization scheme for Hamilton's equations. After a global move, a system that originally had coordinates $\mathbf{r}$ and momenta $\mathbf{p}$ ($\mathbf{r}$,$\mathbf{p}$ denote the coordinates and momenta of all interaction sites in the system) has new trial coordinates $\mathbf{r}^{\text{new}}$ and momenta $\mathbf{p}^{\text{new}}$. Since the system is moved deterministically through phase space, the conditional probability for suggesting configuration $\mathbf{r}^{\text{new}}$ starting at $\mathbf{r}$ depends solely on the momenta at the beginning of the global move. These initial momenta are drawn at random from a Maxwellian distribution of velocities at temperature T before *every* attempted HMC move.

It can be shown[25] that HMC leads to a canonical probability distribution $f_{NVT}(\Gamma)$ provided that the MD part is time-reversible and phase-space volume preserving; the acceptance probability for global moves P is given by

$$P = \min\left[1,\ \exp\left(-\frac{\delta\mathcal{H}}{kT}\right)\right], \tag{8}$$

where H is the full Hamiltonian of the system and $\delta\mathcal{H} = \mathcal{H}^{\text{trial}} - \mathcal{H}^{\text{old}}$ is the difference in the Hamiltonian between trial and original configurations. We note again that neither $f_{NVT}(\Gamma)$ nor any ensemble averages depend on the

size of the time step δt. However, the average acceptance probability $\langle P \rangle$ depends on the average discretization error $\langle \delta \mathscr{H} \rangle$ and therefore depends on δt. For large systems and small time step sizes it can be shown that

$$\langle P \rangle = \mathrm{erfc}\left(\frac{1}{2} \sqrt{\frac{\langle \delta \mathscr{H} \rangle}{kT}} \right) \tag{9}$$

provides a good approximation for the average acceptance probability.[26] Using a given discretization scheme for Hamilton's equations, one is left with two parameters to be varied: the step size δt and the number of integration steps N_{MD} per MC cycle. In the limit $N_{\mathrm{MD}} \to \infty$, the HMC algorithm corresponds to integrating Hamilton's equations. The finite N_{MD} version of HMC corresponds to performing N_{MD} molecular dynamics moves before accepting or rejecting the resulting configuration and randomly refreshing the velocities from a Maxwellian distribution. The time step size δt and the number of MD steps N_{MD} must be tuned to optimize the performance of the algorithm. For the polymer systems studied here, the MD time step sizes can be three times as large as those required for conventional MD at the same temperature and density.

Several publications devoted to the application of HMC for dense polymer melts and long single chains have appeared recently.[27–29] The algorithm has been shown to provide an interesting alternative to more conventional methods for simulation of polymers. A novel generalized-coordinate HMC was suggested by Forrest and Suter[30] and was shown to be 1.5 times faster than molecular dynamics. The hybrid method has also been successfully used for simulation of systems with rapidly varying intermolecular interactions.[31] Note that at low to intermediate density it is more advantageous to use CCB algorithms. Also note that recent extensions of the CCB scheme have permitted simulation of long chain molecules at high packing fractions.[15] Such extensions, however, are relatively new and have not been implemented in this work.

We would also like to stress that in spite of its MD component, HMC remains a Monte Carlo method with all of the advantages of the latter. For example, it can be extended for simulation of open systems.[32] It is also straightforward to maintain a constant pressure or a constant temperature. It can also be used in combination with other MC techniques to optimize the performance of the simulation; as explained in the results section, for our work we combine HMC and ''molecule exchange'' moves to increase efficiency.

We carried out multiple time step hybrid MC simulations on binary blends of 200 chains of various length. Three compositions of 50, 5, and 1 molar percent (100, 10, and 2 chains of component 1) were used in this work. Three different types of blends were studied: purely repulsive blends and full Lennard-Jones blends with the parameters listed in Table I. The intermolecular potential was truncated and shifted at a distance proportional to the Lennard-Jones size parameter σ, to ensure that the potential is exactly zero at the cutoff. The systems simulated here are summarized in Table II. Runs of at least 2000–2400 hybrid MC cycles of 100 multiple time step MD integrations were used in all cases; the first 500–800 MC cycles of each simulation were used for equilibration. Depending on the density, reduced time steps of 0.006–0.011 were employed. Also 5 molecule exchange moves (to be described later) were attempted after each hybrid cycle for the blends with equal size components.

TABLE I. Different types of Lennard-Jones site–site potentials used.

Parameters	Type 1	Type 2	Type 3
Reduced cutoff (relative to σ_{ij})	2.5	2.5	$\sqrt[6]{2}$
Potential shift (relative to ϵ_{ij})	0.016 316 8	0.016 316 8	1.0
σ_{11}	1.0	1.0	1.0
ϵ_{11}	1.0	1.0	1.0
σ_{12}	1.0	1.075	1.15
ϵ_{12}	1.224 744 9	1.224 744 9	1.0
σ_{22}	1.0	1.15	1.3
ϵ_{22}	1.5	1.5	1.0

IV. POLYMER BLEND PRISM

In this section we describe briefly the PRISM equations for polymer blends. Note that these equations are generally applicable; there are no restrictions to the degree of dissimilarity between the two components neither in terms of their chemical structure nor in terms of their chain length. For a binary blend there are three independent total correlation functions $\{h_{11}(r), h_{12}(r), h_{22}(r)\}$, three independent direct correlation functions $\{c_{11}(r), c_{12}(r), c_{22}(r)\}$, two-intramolecular structure factors $\{\omega_1(r), \omega_2(r)\}$, and three independent PRISM equations. Using this notation, a general PRISM equation for a multicomponent polymer mixture in Fourier space can be written as[6]

$$\tilde{\rho}_M \tilde{\rho}_{M'} \hat{h}_{MM'}(k) = \tilde{\rho}_M \hat{\omega}_M(k) \left[\hat{c}_{MM'}(k) \tilde{\rho}_{M'} \hat{\omega}_{M'}(k) + \sum_{M''} \hat{c}_{MM''}(k) \tilde{\rho}_{M'} \tilde{\rho}_{M''} \hat{h}_{M'M''}(k) \right], \tag{10}$$

where $\tilde{\rho}_M$ is the monomer site density of species M. The intramolecular structure factor of species $M, \hat{\omega}_M(k)$, is defined in terms of intramolecular distribution functions between sites α and β $[\hat{\omega}_M^{\alpha\beta}(k)]$ according to

$$\hat{\omega}_M(k) = \frac{1}{N} \sum_{\alpha,\beta} \hat{\omega}_M^{\alpha\beta}(k). \tag{11}$$

TABLE II. Different types of polymer blends used.

Chain length	ρ	T^*	Molar fraction of component 1	Potential
10-mer	0.3	4	0.01	Type 3
	0.6	4	0.01	Type 3
20-mer	0.6	4	0.01	Type 3
	0.6	4	0.05	Type 3
	0.8	4	0.5	Type 1
	0.8	4	0.5	Type 2
50-mer	0.8	4	0.5	Type 1

Given the intramolecular structure factors $\hat{\omega}_1(k)$ and $\hat{\omega}_2(k)$ and some approximate closure relations, the PRISM equations (10) can be solved iteratively for total and direct correlation functions.

In the past, PRISM equations for pure homopolymers or blends have been solved by invoking Flory's ideality hypothesis[33] to determine $\hat{\omega}_M(k)$. We believe, however, that the intermolecular structure of a polymer blend could be intimately coupled to the intramolecular structure of its components. In other words, for polymer blends the problem of self-consistent determination of intra- and intermolecular structure could become important and should be addressed. In this paper we use the self-consistent PRISM formulation of Grayce and Schweizer.[11]

A. Self-consistent PRISM

The self-consistent formulation of PRISM relies on the development of a self-consistent *solvation potential*. A solvation potential reduces the many-body problem of calculating the conformation of a flexible molecule in solution to that of calculating the conformation of a single molecule in an external field. This approach was originally proposed by Chandler and Pratt,[34] who introduced an interaction-site solvation potential such that the conformational behavior of a single solute molecule in its own internal potential plus this solvation potential was approximately the same as the conformational behavior of the same molecule in solution (experiencing full many-molecule interactions). The self-consistent solvation potential is a function of the average structural and thermodynamic properties of the solvent, and therefore depends on density, temperature, composition, and the average conformation of the solvent molecules. In general, the solvation potential is a function of the positions of all N sites on a solute molecule. Just as for the potential energy, it is assumed that this multidimensional function can be represented by a sum of functions of only one variable—intersite separation. In this pairwise-additive approximation the full solvation potential W_N is given by

$$W_N \approx \sum_{\gamma<\lambda}^{N} W_2^{\gamma\lambda}(|\mathbf{r}_\gamma - \mathbf{r}_\lambda|). \tag{12}$$

For homopolymers, further simplifications can be made[35] by setting all $W_2^{\gamma\lambda}(|\mathbf{r}_\gamma - \mathbf{r}_\lambda|)$ equal. In other words, the total potential energy of a single chain under the influence of its environment can be written as a sum over all pair interactions between the sites on the bare chain $U_2^{\gamma\lambda}(r)$ plus the external potential $W_2^{\gamma\lambda}(r)$,

$$U_N^{\text{self}}(r^{3N}) = \sum_{\gamma<\lambda}^{N} [U_2^{\gamma\lambda}(r) + W_2^{\gamma\lambda}(r)]. \tag{13}$$

Several approximate solvation potentials have been proposed in the literature. In this work we use the Percus–Yevick (PY) formulation of Grayce and Schweizer[11] and we merely implement it for blends. This solvation potential has been used in a study of conformation of nonpolar linear polymers[35] and has been shown to capture qualitative trends in the size of macromolecules in a pure polymer melt. To generalize the idea of a solvation potential to the case of multicomponent polymer blends, the matrices of correlation functions and intramolecular structure factors are defined according to

$$\begin{aligned} \hat{H}_{MM'}(k) &\equiv \tilde{\rho}_M \tilde{\rho}_{M'} \hat{h}_{MM'}(k), \\ \hat{\Omega}_{MM'}(k) &\equiv \tilde{\rho}_M \hat{\omega}_M(k)\, \delta_{MM'}, \\ \hat{C}_{MM'}(k) &\equiv \hat{c}_{MM'}(k). \end{aligned} \tag{14}$$

For an m-component blend we define a $m \times m$ matrix of partial structure factors,

$$\hat{\mathbf{S}}(k) = \hat{\Omega}(k) + \hat{\mathbf{H}}(k). \tag{15}$$

In terms of $\hat{\mathbf{S}}(k)$, the solvation potential for component M, $W^{(M)}(r)$, takes the form

$$-\frac{1}{kT} W^{(M)}(r) = \ln\left[1 + \sum_{M''M'''} \int C_{MM''}(|\mathbf{r} - \mathbf{r}'|) \times S_{M''M'''}(|\mathbf{r}' - \mathbf{r}''|) C_{M'''M}(\mathbf{r}'')\, d\mathbf{r}'\, d\mathbf{r}'' \right]. \tag{16}$$

We use the solvation potential (16) to solve polymer blend PRISM equations self-consistently. We will come back to the actual numerical implementation later.

B. Closure approximations

In order to solve the PRISM equations an approximate closure must be provided. For simple atomic liquids a number of closures are available;[2,36] for simple liquids the Percus–Yevick closure is perhaps the most widely used. An atomic PY closure relates the direct correlation functions $c_{MM'}(r)$ to the corresponding total correlation function $h_{MM'}(r)$ via

$$c_{MM'}(r) = [h_{MM'}(r) + 1]\left[1 - \exp \frac{u_{MM'}(r)}{kT} \right], \tag{17}$$

where $u_{MM'}(r)$ is the intersite potential. Until recently, PRISM calculations employed a literal application of atomic closures to site–site correlation functions. Such closures have been found[37] to yield good structural results for hard chains at high densities. Recently, however, it has been argued[43] that when combined with atomic-like closure approximations, PRISM is qualitatively inconsistent with classical mean-field predictions and experimental data of the molecular weight dependence of the critical solution temperature of binary polymer blends. Molecular closures[41,42] apparently correct some of the deficiencies of the theory; these closures predict a linear dependence of the critical temperature on the degree of polymerization, in agreement with classical mean field theory and lattice simulations.[33,43]

To the best of our knowledge, molecular closures have only been implemented for site–site potentials consisting of a hard core part and a slowly varying attractive part. A tentative generalization to continuous potentials has also been outlined[41] although not implemented. The idea is as follows. For a given potential $u_{MM'}(r)$, a formal division of the po-

tential is introduced at a characteristic division point $r^*_{MM'}$. For a homopolymer blend the potential energy is therefore written as

$$u_{MM'}(r) \equiv U_{MM'}(r)\Theta(r^*_{MM'}-r) + V_{MM'}(r)\Theta(r-r^*_{MM'}), \tag{18}$$

where Θ is the Heaviside step function, and $r^*_{MM'}$ can be chosen in a variety of ways, as it is done in perturbation theories for liquids;[2] we use a Barker–Henderson division for the intersite potential. The molecular closure approximation becomes

$$c_{MM'}(r) = [h_{MM'}(r)+1]\left[1-\exp\frac{U_{MM'}(r)}{kT}\right], \quad r<r^*_{MM'}, \tag{19}$$

$$\omega_M * c_{MM'} * \omega_{M'}(r) = \omega_M * [c^{(\mathrm{ref})}_{MM'} + \Delta c_{MM'}] * \omega_{M'}(r), \quad r>r^*_{MM'}, \tag{20}$$

where $*$ denotes a convolution, $c^{(\mathrm{ref})}_{MM'}(r)$ is the direct correlation function of the reference fluid with only continuous repulsive interactions $U_{MM'}(r)$, and $\Delta c_{MM'}(r)$ is an approximate atomic site–site closure relation for the attractive branch of the potential $V_{MM'}(r)$. We propose to relax the existence of a hard-core condition and apply a PY-style ''soft'' molecular closure to an arbitrary continuous potential by setting

$$\Delta c_{MM'}(r) = [h^{(\mathrm{ref})}_{MM'}(r)+1]\left[1-\exp\frac{V_{MM'}(r)}{kT}\right], \quad 0<r<\infty, \tag{21}$$

where $h^{(\mathrm{ref})}_{MM'}(r)$ is the direct correlation function of the reference fluid with only continuous repulsive interactions $U_{MM'}(r)$.

Equation (21), together with Eqs. (19) and (20), define the new molecular PY closure approximation for a continuous potential.

C. Numerical implementation of self-consistent PRISM

The PRISM equation for polymer blends (10) relates the elements of the site–site total correlation functions matrix to those of the site–site direct correlation functions matrix and the matrix elements of the intramolecular structure factors matrix defined by Eq. (14) (via a set of nonlinear integral equations). Given the matrix of intramolecular structure factors $\hat{\Omega}(k)$ and a closure relation, this equation can be solved to obtain $\hat{\mathbf{C}}(k)$ and $\hat{\mathbf{H}}(k)$. Intramolecular structure factors for each component are determined implicitly by the intermolecular structure of the melt through the the solvation potential (16). The determination of the structure of a chain interacting through the full self-consistent pairwise decomposed potential $U^{\mathrm{self}}_N(r^{3N})$ (13) is a complex many-body problem and several approaches have been proposed in the past for its solution.

Schweizer and co-workers[44] used a semiflexible chain model as a reference system to implement an optimized perturbation theory for the intramolecular structure factor of homopolymer chains. A variational approach to the conformation of flexible chains in solution has also been implemented[45] and, more recently, a generating functional method[35] has been proposed. However, all of these methods introduce additional approximations into the theory. Alternatively, the conformational behavior of a chain immersed in a solvation potential can be deduced from a single-chain Monte Carlo simulation.[46] The accuracy of the simulation route is limited only by the amount of cpu time one wishes to spend on the calculation. For reasons discussed in the section on computer simulation, we employ the continuum configurational bias (CCB) technique[13,14] to calculate the intramolecular structure factors of each component of a blend; CCB Monte Carlo simulations are therefore conducted for a chain in its internal potential plus the self-consistent solvation potential induced by the environment.

The actual procedure is implemented as follows: First, we make an initial guess for the intramolecular structure factor matrix $\hat{\Omega}(k)$ and solve PRISM equations for the intermolecular structure of the blend. We use Eq. (16) to obtain an initial guess for the solvation potentials of each component $W^{(M)}(r)$; a CCB simulation is then conducted for a single chain of each component in these potentials to arrive at new values for $\hat{\Omega}(k)$. Additional details on the calculations using the new molecular PY-style closure for an arbitrary continuous potential are given in Appendix B.

V. RESULTS AND DISCUSSION

A. HMC simulation results

As already pointed out, it is difficult to obtain accurate structural information for dense polymers using conventional simulation techniques. For polymer blends we also confront the problem of obtaining the correct compositional distribution. Due to the high molecular weight and the chain structure, the mobility of a polymer molecule is extremely small, thus preventing us from efficiently sampling possible interchain rearrangements in a reasonable amount of cpu time. One of the goals of this work was the development of an efficient simulation code for simulating dense polymers. By the efficiency of the simulation algorithm we imply its ability to eliminate correlations between successive configurations. As an indicator of such efficiency, we consider the decay of the bond vector autocorrelation function, defined by

$$C_{bb}(t) = \left\langle \frac{\mathbf{l}(0)\cdot\mathbf{l}(t)}{|\mathbf{l}(0)||\mathbf{l}(t)|} \right\rangle, \tag{22}$$

where $\mathbf{l}(t)$ is the orientation of a bond vector at time t. The brackets denote an average over all bonds in the system and over many successive configurations of the system. This function provides a measure of segmental mobility and follows the overall rotation of bonds on a chain. In the melt, the probability distribution of any given bond vector should be isotropic; any efficient algorithm should therefore be capable of erasing the ''memory'' of the bond orientation in as few computational steps as possible. Two configurations that are

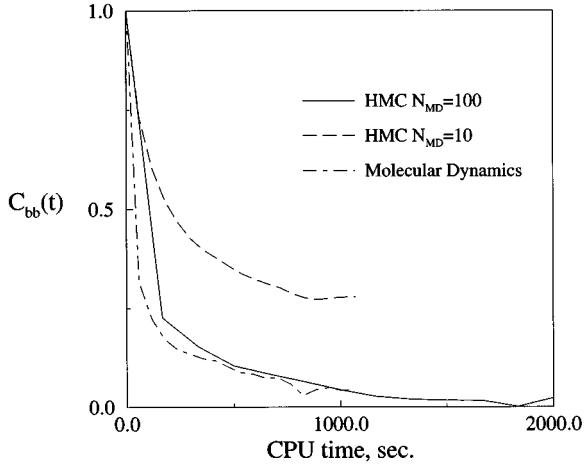

FIG. 1. Bond vector correlation function (22) for a system of Lennard-Jones 10-mers. Site number density $\rho=0.6$, reduced temperature $T^*=4$, reduced MD time step $\delta t=0.01$. The solid line corresponds to 100 MD steps per MC cycle, the dashed line corresponds to 10 MD steps per MC cycle, and the dot–dashed line corresponds to a multiple time step MD simulation with $\delta t=0.006$.

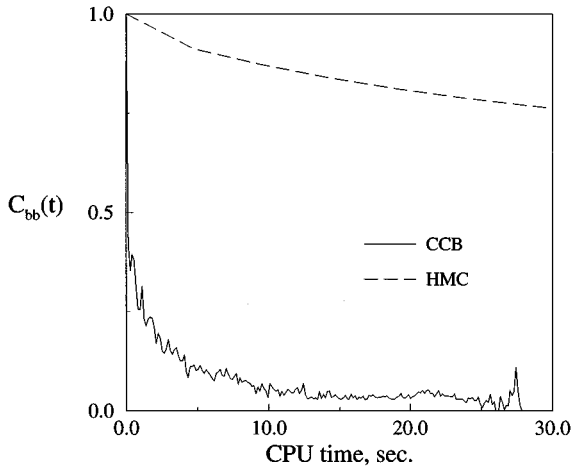

FIG. 2. Bond vector correlation function (22) for a single chain of length 100. The solid line shows results of a CCB simulation, and the dashed line shows results of a HMC simulation with 100 MD steps per MC cycle and $\delta t=0.01$.

separated by cpu time t in the sequence are only truly independent if $C_{bb}(t)\approx 0$. Achieving $C_{bb}(t)\rightarrow 0$ for small t is one of the main challenges facing a molecular simulation algorithm.

Two parameters can be used to maximize the efficiency of the HMC algorithm. First, one can use different numbers of MD time steps per MC cycle. It turns out that this parameter dramatically affects the performance of the method. Figure 1 shows the results for the bond autocorrelation function $C_{bb}(t)$ in a melt of 10-mers for two different values of N_{MD} along with those for molecular dynamics calculations. It is clear that using large N_{MD} favors a faster rate of correlations decay. However, increasing N_{MD} leads to more expensive HMC moves; we believe that $N_{\mathrm{MD}}\sim 100$ is about the optimum choice for HMC simulations of chains of intermediate length. For large N_{MD} the HMC method is very similar to the MD method. As shown in Fig. 1, for $N_{\mathrm{MD}}=100$ the performances of HMC and MD are comparable.

Further comments are needed on Fig. 1. One of the reasons why we consider HMC to be superior for our work is that it allows for the use of large time steps in the MD part of the algorithm while keeping the temperature constant through the MC acceptance criterion. We prefer to use HMC in conjunction with multiple time scales because at this point we are still uncertain as to the time steps that can be used in multiple time step MD without introducing errors into the results; HMC is just a safer and equally efficient method, the temperature and the pressure are easy to control, and it is possible to combine it with several other Monte Carlo techniques to push the performance even further. We have, for example, implemented identity interchange moves to speed convergence. In these moves, a chain of species M and a chain of species M', chosen at random, exchange identities, thereby circumventing some of the diffusional limitations encountered in conventional MD.

We also considered the possibility of using HMC for simulations of a single chain in an external potential. The efficiency of these simulations is of great importance since they are used in the self-consistent formulation of PRISM. We have performed efficiency tests on single chains of 100 and 200 segments. Figure 2 shows results for $C_{bb}(t)$ for a 100-mer using HMC and CCB methods. Clearly, CCB is superior to HMC by several orders of magnitude. The same is also true for 200-mers. This makes the CCB technique a valuable tool for single chain simulations in external potentials; we take advantage of its performance in our self-consistent PRISM calculations.

B. PRISM results

The polymer RISM equation (10) has been solved with the standard atomic-like PY closure for purely repulsive blends (Type 3, see Table I); for attractive chains of type 1 and type 2, the new molecular PY closure for continuous potentials has also been applied.

We employed two different approaches to determine the intramolecular structure of the components of a blend. In the first, the intramolecular structure $\hat{\Omega}(k)$ was obtained directly from many-chain HMC simulations, and inserted as an input into Eq. (10). In this case, the results provide an unambiguous test of the ability of PRISM to capture the local structure of a blend. Such tests have been carried out for various types of blends, compositions, and site number densities ρ.

We begin by comparing the cross total correlation function $h_{12}(r)$, predicted by PRISM from simulated intramolecular structure factors $\omega_i(r)$ for a binary blend of repulsive 10-mers of type 3 to our results of HMC simulations [Fig. 3(a)]. The calculations have been carried out at an intermediate site number density of $\rho=0.3$ ($\rho=N_{\mathrm{sites}}/V$) and a very low molar fraction ($x_1=0.01$) of the component with a smaller segment size. The segment size of the second component was 33% larger than that of the first component. Figure 3(b) shows the results for total correlation functions for the same blend of repulsive 10-mers at a much higher site

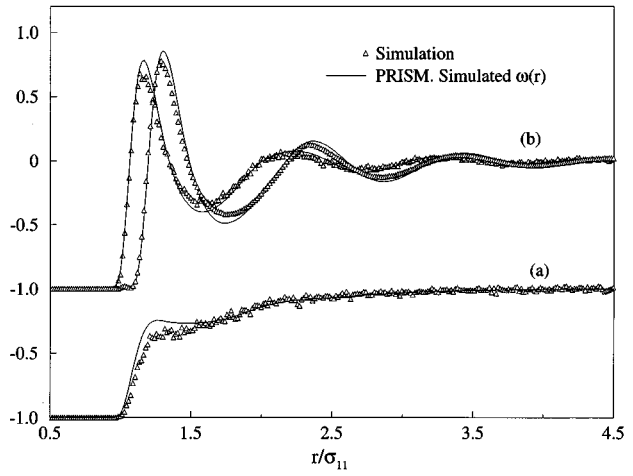

FIG. 3. (a) The 1-2 total correlation function for a blend of repulsive 10-mers of type 3 at site number density $\rho=0.3$ (see Table II). (b) The 1-2 and 2-2 total correlation functions for a blend of repulsive 10-mers of type 3 at site number density $\rho=0.6$ (see Table II). The triangles show results of simulations; the solid line was predicted by PRISM from the simulated intramolecular distribution functions $\omega(r)$.

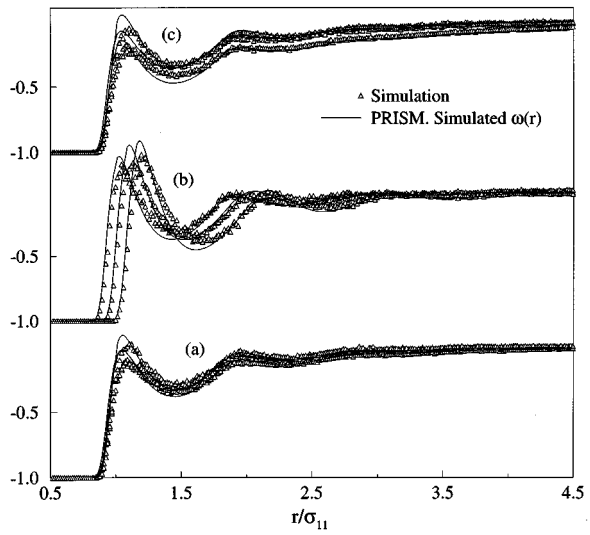

FIG. 5. (a) The 1-1, 1-2, and 2-2 total correlation functions for a blend of attractive 20-mers of type 1 (see Table II). (b) The 1-1, 1-2, and 2-2 total correlation functions for a blend of attractive 20-mers of type 2 (see Table II). (c) The 1-1, 1-2, and 2-2 total correlation functions for a blend of attractive 50-mers of type 1 (see Table II). The triangles show simulation results; the solid line was predicted by PRISM from simulated intramolecular distribution functions $\omega(r)$ with a Percus–Yevick molecular closure.

number density [$\rho=0.6$; only $h_{12}(r)$ and $h_{22}(r)$ are shown]. Note that the local structure of the blend is captured almost quantitatively by the theory. Having shown the accuracy of the formalism for repulsive 10-mers at infinite dilution, we turn our attention to longer repulsive chains and slightly higher concentrations of the small-segment component. Figure 4(a) shows $h_{12}(r)$ and $h_{22}(r)$ for a blend of 20-mers of type 3 at $\rho=0.6$ and $x_1=0.01$. Again the results are encouraging. Note that the curves on Figs. 3(b) and 4(a) look very similar but the correlation hole effect is more pronounced in the case of 20-mers. From Fig. 4(b) we also conclude that changing the molar fraction of the first component from 0.01 to 0.05 does not change the structure of the blend appreciably and the accuracy of the theoretical predictions is preserved. As already shown by Stevenson *et al.*,[9] we also find that for purely repulsive blends the theory captures all the basic features of local packing and agreement with simulations is quantitative. These results are in contrast to our earlier calculations at somewhat lower densities.[10]

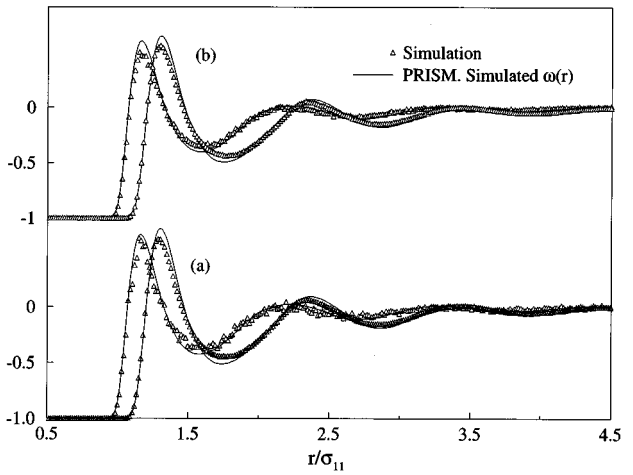

FIG. 4. (a) The 1-2 and 2-2 total correlation functions for a blend of repulsive 20-mers of type 3; the mole fraction of component 1 is 0.01 (see Table II). (b) The 1-2 and 2-2 total correlation functions for a blend of repulsive 20-mers of type 3; the mole fraction of component 1 is 0.05 (see Table II). The triangles show simulation results; the solid line was predicted by PRISM from simulated intramolecular distribution functions $\omega(r)$.

We now proceed to discuss results for attractive chains. We use a new molecular closure for continuous potentials to determine the structure of attractive polymer blends. Figure 5(a) shows theoretical predictions and simulation results for all three total correlation functions for a blend of attractive 20-mers of type 1. For this system, the site number density was $\rho=0.8$, the reduced temperature was $T^*=4$, and the molar fraction was $x_1=0.5$. To separate the effects of ''size'' and ''energy'' dissimilarities, the sizes of the segments were equal for both components. In this case the theory is slightly off around the first peak, but the overall agreement is still satisfactory. Next, we investigate a blend under the same conditions, but with both types of dissimilarity present. This is the most general case. The results of such a calculation are shown in Fig. 5(b); the agreement between theoretical and simulated results is satisfactory for all three correlation functions.

Encouraged by these results, we attempted simulations of 50-mer blends under similar conditions. Since identity exchange moves become ineffective for chains having different segment sizes, we only present results for a blend of 50-mers of type 1. Calculations have been carried out for this system at a number site density of $\rho=0.8$, a reduced temperature $T^*=4$, and equimolar composition. Our results [Fig. 5(c)] indicate that the overall agreement between theory and simulation for long chains is still satisfactory.

In summary, we find that PRISM gives an adequate de-

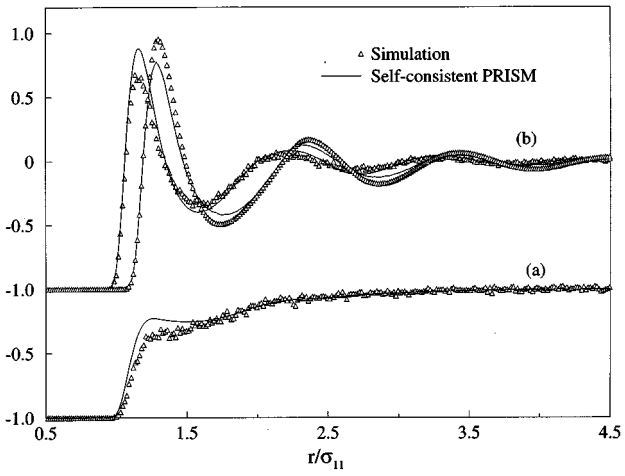

FIG. 6. (a) The 1-2 total correlation function for a blend of repulsive 10-mers of type 3 at the site number density $\rho=0.3$ (see Table II). (b) The 1-2 and 2-2 total correlation functions for a blend of repulsive 10-mers of type 3 at the site number density $\rho=0.6$ (see Table II). The triangles show simulation results; the solid line was predicted by self-consistent PRISM.

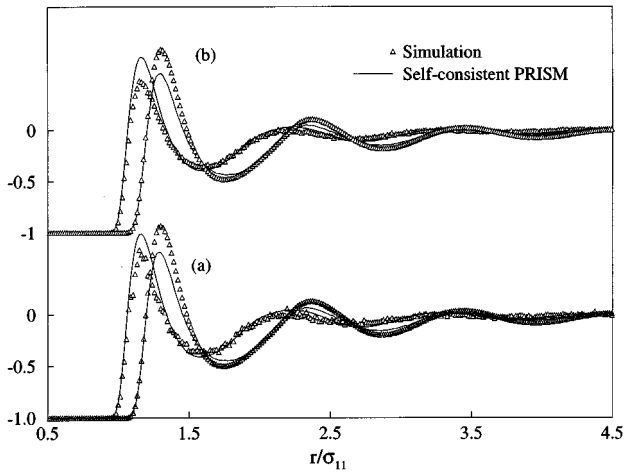

FIG. 7. (a) The 1-2 and 2-2 total correlation functions for a blend of repulsive 20-mers of type 3; the mole fraction of component 1 is 0.01 (see Table II). (b) The 1-2 and 2-2 total correlation functions for a blend of repulsive 20-mers of type 3; the mole fraction of component 1 is 0.05 (see Table II). The triangles show simulation results; the solid line was predicted by self-consistent PRISM.

scription of the structure of various binary blends. For the case of attractive blends, however, the theory seems to slightly overestimate the role of attractive forces on the local structure. Also note that for the systems of attractive chains studied in this work we did not find a significant difference between the results obtained with different types of closures. However, any such differences (between molecular and atomic closures) could become noticeable at temperatures below those investigated in this work.

Provided the average intramolecular structure of both components is known, PRISM provides an accurate formalism for description of the intermolecular structure of polymer blends. From a practical point of view, however, this formalism is not of immediate use because single chain structure factors must be determined from many-chain simulations. This problem is circumvented by utilizing the self-consistent formulation of PRISM; we compare our self-consistent predictions for the structure of the blends described above to results of simulations. Figures 6(a) and 6(b) show self-consistent total correlation functions together with those obtained from simulation for a system of 10-mers [see also Figs. 3(a) and 3(b)]. We see that the self-consistent results are almost identical to those obtained from simulated intramolecular structures. We do find, however, that the deficiency of the theory around the first peak is slightly enhanced. The same is true for the systems in Figs. 7(a)–8(c) [these are identical to the systems in Figs. 3(a)–5(c)].

We conclude that, for the self-consistent formulation employed in this work, agreement with simulations is perhaps not as good as when a simulated intramolecular structure is employed, but it is still highly satisfactory.

VI. CONCLUSIONS

A hybrid multiple time step Monte Carlo algorithm has been successfully used to simulate dense polymer blends. The method combines the advantages of molecular dynamics and Monte Carlo techniques. A multiple time step molecular dynamics scheme has been employed as a part of the hybrid algorithm. While the autocorrelation times for latter method are of the same order of magnitude as in multiple time step MD, the hybrid algorithm is exact and can be combined with other MC techniques. In this work, a molecule identity interchange move has been implemented to circumvent the diffusional limitations of the MD method for long molecules.

The results of our simulations have been used to examine the predictions of polymer RISM theory. We have studied the structure of polymer blends of various types over a broad

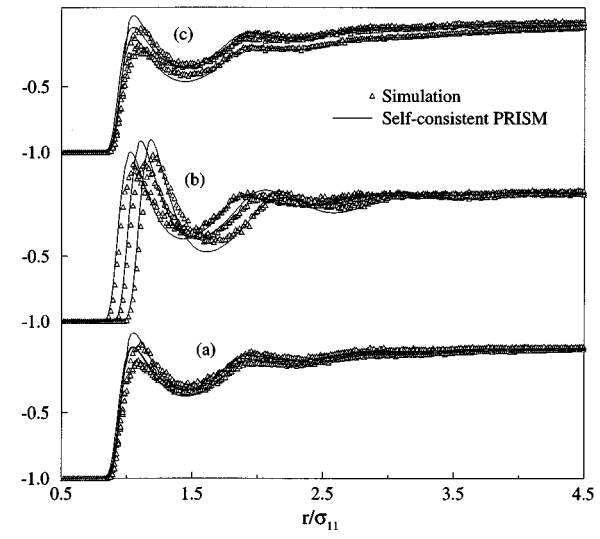

FIG. 8. (a) The 1-1, 1-2, and 2-2 total correlation functions for a blend of attractive 20-mers of type 1 (see Table II). (b) The 1-1, 1-2, and 2-2 total correlation functions for a blend of attractive 20-mers of type 2 (see Table II). (c) The 1-1, 1-2, and 2-2 total correlation functions for a blend of attractive 50-mers of type 1 (see Table II). The triangles are simulation results; the solid line was predicted by self-consistent PRISM with a Percus–Yevick molecular closure.

range of chain lengths and densities. Both purely repulsive and attractive blends have been investigated. A new molecular closure has been applied for attractive blends and a newly developed self-consistent formulation of PRISM (that does not require prior knowledge of the intramolecular structure of the components) has been implemented. We find that PRISM predictions using simulated intramolecular structure factors are in very good agreement with simulated data. We also find that the predictions of self-consistent PRISM are almost identical to those obtained from simulated intramolecular structure factors. We conclude that the self-consistent formulation of the theory studied in this work provides a useful formalism for studying the molecular structure of simple binary polymer blends.

ACKNOWLEDGMENTS

The authors are grateful to J. Curro and J. McCoy for sending us a reprint of their work (Ref. 9) prior to publication. This work was supported by the National Science Foundation and by the donors of the Petroleum research fund administered by the American Chemical Society.

APPENDIX A: MULTIPLE TIME STEP MD IMPLEMENTATION

We divide the force acting on each interaction site i into two parts: one arising from interactions with neighboring covalently bonded sites on the same chain ($\mathbf{F}_i^{\text{strong}}$) and another one arising from to all other Lennard-Jones interactions ($\mathbf{F}_i^{\text{weak}}$). We introduce two time steps, dt^{small} and $dt^{\text{large}}=dt^{\text{small}}\cdot N$, where N is an arbitrary integer which depends on the ratio of two characteristic time scales of the system. We use $N=10$ for our work. With this division the algorithm becomes

(1) Advance all velocities using $\mathbf{F}_i^{\text{weak}}$ only,

$$\mathbf{v}_i=\mathbf{v}_i+0.5dt^{\text{large}}\mathbf{F}_i^{\text{weak}}.$$

(2) Perform the standard velocity Verlet[47] algorithm iteratively N times using $\mathbf{F}_i^{\text{strong}}$ only.
(3) Calculate new $\mathbf{F}_i^{\text{weak}}$.
(4) Complete the move using

$$\mathbf{v}_i=\mathbf{v}_i+0.5dt^{\text{large}}\mathbf{F}_i^{\text{weak}}.$$

APPENDIX B: MOLECULAR CLOSURE NUMERICAL PROCEDURE

This appendix describes the iterative procedure that we use to solve PRISM with the new molecular closure for the case of a continuous site–site potential.

Equations (18)–(21) define this closure approximation. We consider the case of a pure polymer, but our discussion can be generalized to multicomponent systems in a systematic manner. For this case the PRISM equation is[3,4]

$$\hat{h}(k)=\hat{\omega}(k)\hat{c}(k)\hat{\omega}(k)+\rho_m\hat{\omega}(k)\hat{c}(k)\hat{h}(k). \tag{B1}$$

The potential can be divided in several ways; we used the standard Barker–Henderson[2] division, thus defining a reference potential $U(r)$ and a perturbation $V(r)$.

We first solve the PRISM equation (B1) for the reference system having only a repulsive potential $U(r)$ for the functions $h^{(\text{ref})}(r)$ and $c^{(\text{ref})}(r)$, $0<r<\infty$. $\Delta c(r)$ is then calculated from Eq. (21) with $V_{MM'}(r)=V(r)$ and the ''outer part'' of convolution $\omega*c*\omega(r)$ is calculated from

$$\omega*c*\omega(r)=\omega*[c^{(\text{ref})}(r)+\Delta c(r)]*\omega(r), \quad r>r^*. \tag{B2}$$

This ''outer part'' is fixed throughout further calculations. We define an auxiliary function by

$$\gamma(r)=h(r)-\omega*c*\omega(r), \quad 0<r<\infty \tag{B3}$$

with $h(r)$ and $c(r)$ being the current functions at every iteration loop. An initial guess for $\gamma^{(0)}(r)=h^{(\text{ref})}(r)-\omega*c^{(\text{ref})}*\omega(r)$, $(0<r<\infty)$ is made.

Re-expressing the closure (19) in terms of $\gamma(r)$ gives

$$\omega*c*\omega(r)=\frac{c(r)}{1-\exp[U(r)/kT]}-\gamma(r)-1, \quad r<r^* \tag{B4}$$

which is not analytically solvable for $c(r)$. We solve (B4) iteratively for $c(r)$ and $\omega*c*\omega(r)$ simultaneously [using the previously calculated ''outer part'' of $\omega*c*\omega(r)$] through a Picard iteration scheme. An initial guess for the ''inner part'' of convolution $\omega*c*\omega(r)$ is made,

$$\omega*c*\omega(r)=\omega*c^{(\text{ref})}*\omega(r), \quad r<r^*. \tag{B5}$$

The convolution $\omega*c*\omega(r)$ is then transformed and $\hat{c}(k)$ and $c(r)$ are calculated. Inserting $c(r)$ into Eq. (B4) we get a new guess for $\omega*c*\omega(r)$ for $r<r^*$. The iteration loop is repeated until convergence is achieved. As a result we have a new $\omega*c*\omega(r)$ for $0<r<\infty$.

This function is used to calculate a new guess for $h(r)$ through Eq. (B3). This function is then inserted in Eq. (B1) to get a new guess for the auxiliary function $\gamma^{(1)}(r)$. This function replaces $\gamma^{(0)}(r)$ as an input to the next iteration in which the next approximations to the ''inner part'' of $\omega*c*\omega(r)$ and $c(r)$ are obtained. The procedure is repeated until $\gamma(r)$ is no longer changing. As it is often the case, it is necessary to mix successive solutions[2] for the procedure to converge.

[1] S. A. Rice and P. Gray, *The Statistical Mechanics of Simple Liquids* (Interscience, New York, 1965).
[2] J.-P. Hansen and I. R. McDonald, *Theory of Simple Liquids* (Academic, New York, 1986).
[3] K. S. Schweizer and J. G. Curro, Phys. Rev. Lett. **58**, 246 (1987).
[4] J. G. Curro and K. S. Schweizer, J. Chem. Phys. **87**, 1842 (1987).
[5] J. G. Curro and K. S. Schweizer, Macromolecules **20**, 1928 (1987).
[6] K. S. Schweizer and J. G. Curro, J. Chem. Phys. **91**, 5059 (1989).
[7] K. S. Schweizer and J. G. Curro, Phys. Rev. Lett. **60**, 809 (1988).
[8] J. G. Curro and K. S. Schweizer, J. Chem. Phys. **88**, 7242 (1988).
[9] C. S. Stevenson, J. G. Curro, J. D. McCoy, and S. J. Plimpton, J. Chem. Phys. **103**, 1208 (1995).
[10] J. J. de Pablo, in *Lectures on Thermodynamics and Statistical Mechanics*, edited by M. L. de Haro and C. Varea (World Scientific, Singapore, 1994).
[11] C. J. Grayce and K. S. Schweizer, J. Chem. Phys. **100**, 6846 (1994).
[12] H. R. Warner, Jr., Ind. Eng. Chem. Fundamentals **11**, 379 (1972).
[13] J. J. de Pablo, M. Laso, and U. W. Suter, J. Chem. Phys. **96**, 2395 (1992).
[14] J. J. de Pablo, M. Laso, and U. W. Suter, J. Chem. Phys. **96**, 6157 (1992).
[15] F. Escobedo and J. J. de Pablo, J. Chem. Phys. **102**, 2636 (1995).
[16] F. Escobedo and J. J. de Pablo, Macromol. Theory Simul. **4**, 691 (1995).
[17] F. Escobedo and J. J. de Pablo, J. Chem. Phys. **103**, 2703 (1995).

[18] E. Leontidis, J. J. de Pablo, M. Laso, and U. W. Suter, in *Advances in Polymer Science* (Springer, Berlin, 1994), Vol. 116.
[19] M. E. Tuckerman, G. J. Martyna, and B. J. Berne, J. Chem. Phys. **93**, 1287 (1990).
[20] M. E. Tuckerman and B. J. Berne, J. Chem. Phys. **94**, 6811 (1991).
[21] M. E. Tuckerman, B. J. Berne, and G. J. Martyna, J. Chem. Phys. **97**, 1990 (1992).
[22] D. J. Evans and G. P. Morriss, *Statistical Mechanics of Nonequilibrium Liquids* (Academic, New York, 1990).
[23] J. J. Erpenbeck and W. W. Wood, in *Statistical Mechanics B. Modern Theoretical Chemistry*, edited by B. J. Berne (Plenum, New York, 1977), Vol. 6.
[24] S. Duane, A. D. Kennedy, B. J. Pendelton, and D. Roweth, Phys. Lett. B **195**, 216 (1987).
[25] B. Mehlig, D. W. Heerman, and B. M. Forrest, Phys. Rev. B **45**, 679 (1992).
[26] S. Gupta, A. Irbäck, F. Karsch, and B. Petersson, Phys. Lett. B **242**, 437 (1988).
[27] D. W. Heerman and L. Yixue, Macromol. Chem. Theory Simul. **2**, 229 (1993).
[28] B. M. Forrest and U. W. Suter, J. Chem. Phys. **101**, 2616 (1994).
[29] A. Irbäck, J. Chem. Phys. **101**, 1661 (1994).
[30] B. M. Forrest and U. W. Suter, Mol. Phys. **82**, 393 (1994).
[31] F. A. Brotz and J. J. de Pablo, Chem. Eng. Sci. **49**, 3015 (1994).
[32] J. J. de Pablo, Fluid Phase Equilib. **104**, 195 (1995).
[33] P.-G. de Gennes, *Scaling Concepts in Polymer Physics* (Cornell University, Ithaca, 1979).
[34] D. Chandler and L. R. Pratt, J. Chem. Phys. **65**, 2925 (1976).
[35] C. J. Grayce, A. Yethiraj, and K. S. Schweizer, J. Chem. Phys. **100**, 6857 (1994).
[36] G. A. Martynov and G. N. Sarkisov, Mol. Phys. **49**, 1495 (1983).
[37] A. Yethiraj and K. S. Schweizer, J. Chem. Phys. **97**, 1455 (1992).
[38] K. S. Schweizer and J. G. Curro, J. Chem. Phys. **91**, 5059 (1989).
[39] J. G. Curro and K. S. Schweizer, Macromolecules **23**, 1402 (1990); **24**, 6736 (1991).
[40] K. S. Schweizer and J. G. Curro, Chem. Phys. **149**, 105 (1990).
[41] K. S. Schweizer and A. Yethiraj, J. Chem. Phys. **98**, 9053 (1993).
[42] A. Yethiraj and K. S. Schweizer, J. Chem. Phys. **98**, 9080 (1993).
[43] H. P. Deutsch and K. Binder, Europhys. Lett. **17**, 697 (1992); Macromolecules **25**, 6214 (1992).
[44] K. S. Schweizer, K. G. Honnel, and J. G. Curro, J. Chem. Phys. **96**, 3211 (1992).
[45] J. Melenkevitz, J. G. Curro, and K. S. Schweizer, J. Chem. Phys. **99**, 5571 (1993).
[46] J. Melenkevitz, K. S. Schweizer, and J. G. Curro, Macromolecules **26**, 6190 (1993).
[47] M. P. Allen and D. J. Tildesley, *Computer Simulation of Liquids* (Clarendon, Oxford, 1989).